RESEARCH REPORT

Slit cleavage is essential for producing an active, stable, non-diffusible short-range signal that guides muscle migration

Elly Ordan[1], Marko Brankatschk[2,*], Barry Dickson[2,‡], Frank Schnorrer[2,§] and Talila Volk[1,¶]

ABSTRACT

During organogenesis, secreted signaling proteins direct cell migration towards their target tissue. In *Drosophila* embryos, developing muscles are guided by signals produced by tendons to promote the proper attachment of muscles to tendons, essential for proper locomotion. Previously, the repulsive protein Slit, secreted by tendon cells, has been proposed to be an attractant for muscle migration. However, our findings demonstrate that through tight control of its distribution, Slit repulsion is used for both directing and arresting muscle migration. We show that Slit cleavage restricts its distribution to tendon cells, allowing it to function as a short-range repellent that directs muscle migration and patterning, and promotes their halt upon reaching the target site. Mechanistically, we show that Slit processing produces a rapidly degraded C-terminal fragment and an active, stable N-terminal polypeptide that is tethered to the tendon cell membrane, which further protects it from degradation. Consistently, the requirement for Slit processing can be bypassed by providing an uncleavable, membrane-bound form of Slit that is stable and is retained on expressing tendon cells. Moreover, muscle elongation appears to be extremely sensitive to Slit levels, as replacing the entire full-length Slit with the stable Slit-N-polypeptide results in excessive repulsion, which leads to a defective muscle pattern. These findings reveal a novel cleavage-dependent regulatory mechanism controlling Slit spatial distribution, which may operate in other Slit-dependent processes.

KEY WORDS: Slit, Slit cleavage, Muscle, Muscle migration, Tendon

INTRODUCTION

Muscle migration and adhesion to tendon cells represents a key process that is essential for the establishment of functional contractile tissues in vertebrate and invertebrate organisms (Schejter and Baylies, 2010; Schnorrer and Dickson, 2004; Schweitzer et al., 2010). To achieve precise encounter between muscles and tendons, muscles communicate with tendon cells during their elongation and adhesion (Bökel and Brown, 2002; Schweitzer et al., 2010). The mechanism directing muscle elongation and their further arrest is not clear.

Slit has been described previously to function in *Drosophila* muscle migration (Kramer et al., 2001; Wayburn and Volk, 2009). Slit is expressed by tendon cells and has been shown to exhibit dual and opposite activities. At early developmental stages, it repels the

[1]Department of Molecular Genetics, Weizmann Institute of Science, Rehovot 76100, Israel. [2]Institute of Molecular Pathology (IMP), Vienna A-1030, Austria. *Present address: Max Planck Institute of Molecular Cell Biology and Genetics, Dresden, Germany. ‡Present address: Janelia Farm Research Campus, Howard Hughes Medical Institute, 19700 Helix Drive, Ashburn, VA 20147, USA. §Present address: Max Planck Institute of Biochemistry, 82152 Martinsried, Germany.
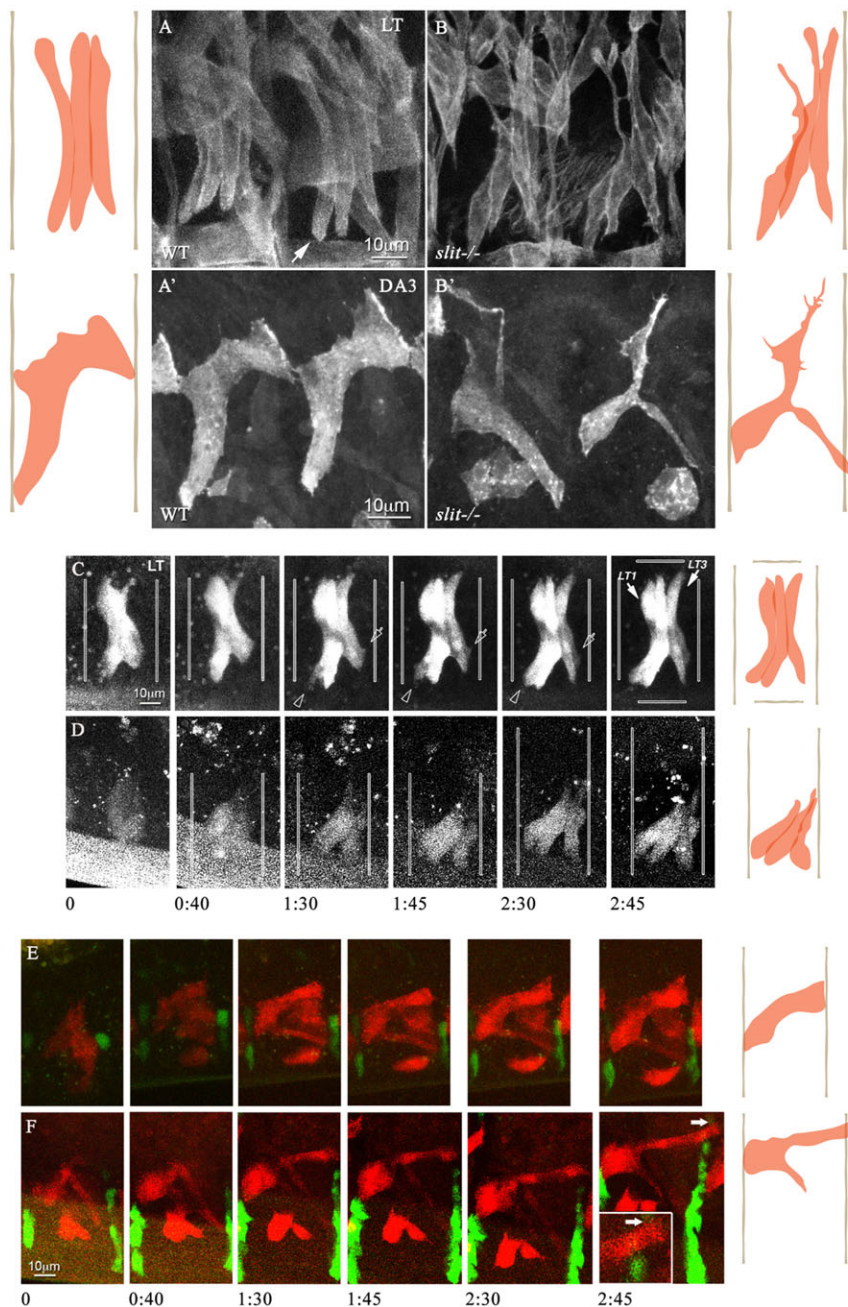
¶Author for correspondence (talila.volk@weizmann.ac.il)

ventral longitudinal muscles at the ventral midline, whereas at later developmental stages, it attracts these muscles at the segmental borders (Kramer et al., 2001).

Slit is a large secreted multi-domain protein consisting of leucine-rich repeats (LRR), followed by multiple EGF repeats and a C-terminal cysteine knob. Structure-function analysis demonstrated that the binding site for its receptor, Roundabout (Robo), resides in the second LRR domain located at the N-terminal region (Brose et al., 1999; Kidd et al., 1999; Rothberg and Artavanis-Tsakonas, 1992; Rothberg et al., 1988, 1990). In both flies and vertebrates, Slit proteins undergo cleavage into a large N-terminal fragment, Slit-N, which contains the Robo-binding site, and a shorter C-terminal fragment (Slit-C) (Brose et al., 1999; Wang et al., 1999). The contribution of Slit cleavage to its function as a guide molecule has yet to be elucidated. Experiments in cultured rat dorsal root ganglia and with olfactory bulb neurons suggested that Slit-N stimulates axon branching, whereas full-length Slit (Slit-FL) inhibits branching activity (Nguyen Ba-Charvet et al., 2001). In the *Drosophila* CNS, both Slit-uncleavable (Slit-UC) and Slit-FL were capable of rescuing the *slit* mutant phenotype (Coleman et al., 2010); thus, the functional relevance of Slit cleavage is as yet unclear.

We analyzed the contribution of Slit to muscle migration by performing live imaging of embryos mutant for *slit,* as well as embryos in which the uncleavable forms of Slit were knocked into the *slit* locus. We demonstrate that Slit cleavage is essential for Slit-mediated short-range repulsion and arrest of muscle migration, and propose that this mechanism might be essential for Slit short-range signaling in other tissues, including heart and blood vessels.

RESULTS AND DISCUSSION

Slit is essential for correct orientation of both DA3 and LT muscles, and for arresting their elongation

To study the role of Slit in muscle migration, we analyzed individual muscles with different orientations that can be visualized in live and fixed *Drosophila* embryos. These included the three lateral transverse (LT) muscles and the dorsal acute muscle 3 (DA3) (Fig. 1). Results showed that the pattern of these muscles in *slit* mutants was significantly aberrant. The LT muscles were oriented diagonally instead of vertically and were closer to the segmental border, where Slit is normally present (Fig. 1B,D). Quantification of the distance between the LT3 muscle and the posterior segment border (D_{LT3}) relative to the width of the hemisegment (D_s) revealed a 60% reduction in the mutant [D_{LT3}/D_s=0.149±0.05 in *slit* relative to 0.249±0.06 in wild type (WT), P=0.001]. The DA3 muscle often splits into two misoriented extensions in the *slit* mutants (Fig. 1B′,F) and, importantly, it continued to elongate beyond its target tendons (Fig. 1E,F).

Live imaging of wild-type GFP-labeled LT muscles indicated that they elongated in a dorsoventral direction, and often sent small membrane extensions reaching laterally to the segmental border

Fig. 1. Slit is essential for correct patterning of both DA3 and LT muscles. (A-B′) Orientation of LT muscles visualized with anti-tropomyosin (A,B) or of DA3 muscle visualized with Collier-GFP (A′,B′) in wild type (WT, A,A′) or in *slit* mutant (B,B′) embryos at stage 16. The outlines of the corresponding muscles relative to the segment borders are shown. Arrow in A indicates smooth surfaces of the LT1 muscle. (C,D) Live imaging of wild type (C) or *slit* mutant (D) of GFP-labeled LT muscles during their elongation towards tendons located at the center of the segment. Small membrane extensions are marked by empty arrowheads or arrows in C,D. (E,F) The DA3 muscle is marked by *col>GFP* and *Sr>DsRED*. Arrows indicate a muscle that does not stop when it reaches the targeted tendon cell. Scale bars: 10 µm.

(Fig. 1C; supplementary material Movie S1). Once the LT muscles reached their target tendons, their surfaces became smooth (e.g. see Fig. 1A, arrow). *In vivo* imaging of *slit* mutant embryos showed that the LT muscles were often diagonally misoriented (Fig. 1D; supplementary material Movie S2), a phenotype consistent with loss of repulsion cues from the segment border cells. *In vivo* imaging of *slit* mutant embryos expressing a GFP-labeled DA3 muscle and stripe-RFP-labeled segment border cells indicated that in addition to splitting, the muscle often failed to stop at the segment border, crossing the Slit-expressing tendon cells (Fig. 1F, arrow; supplementary material Movies S3 and S4). Notably, prior to their migration, the pattern of these muscles appeared similar to that of wild-type muscles (supplementary material Movies S1 and S2). These results indicate that Slit is needed to direct the muscles to the correct route and to arrest their extension once they reach the attachment site, but it is not required for their initial patterning.

Slit cleavage is essential for the induction of normal muscle pattern

In both flies and vertebrates, Slit proteins undergo cleavage into a large N-terminal fragment termed Slit-N, which contains the Robo-binding site, and a shorter C-terminal fragment (Slit-C) (Brose et al., 1999; Wang et al., 1999). To address the contribution of Slit cleavage to the induction of muscle extension, we used flies carrying knock-in cleavable and uncleavable versions inserted into the *slit* locus by homologous recombination (supplementary material Fig. S1). In these mutants, all the DNA and RNA regulatory sequences were present and only the cleavage site was replaced by mutant sequences, and a myc tag was fused to the C-terminus. Analysis showed that Slit-FL-myc rescued the LT muscle phenotype, as 13% of affected segments were seen in the rescue relative to 77% in *slit* mutant (P=0.0001, n=18). In addition, the D_{LT3}/D_s ratio improved to wild-type levels (D_{LT3}/D_s=0.21±0.03 in

Slit-FL-myc, relative to 0.149±0.03 in *slit*, *P*=0.008). Improvement was also observed in the DA3 muscle of Slit-FL-myc embryos, as 4% affected segments were seen in the rescue relative to 50% in *slit* mutant (*P*=0.00009, *n*=21) (Fig 2B,B′). By contrast, the uncleavable form of Slit (Slit-UC-myc), which lacks the cleavage site, did not rescue the phenotype of either the LT or DA3 *slit* mutant muscles (Fig. 2C,C′), and its D_{LT3}/D_s ratio was 0.107±0.06. Notably, a membrane-bound version of the Slit-UC-myc (Slit-UC-CD8-myc) carrying a CD8 domain at the Slit C-terminal did rescue the LT muscle phenotype, as only 42% of the segments showed a phenotype, relative to 77% in the *slit* mutant (*P*=0.0093, *n*=18). The D_{LT3}/D_s ratio in this case was 0.28±0.05, closely similar to control. For the DA3 muscle, 5% of the segments were affected relative to 50% in *slit* mutants (*P*=0.00004, *n*=21) (Fig. 2D,D′). Slit cleavage is therefore essential for guiding the elongation of the LT and DA3 muscles; however, it is dispensable once Slit is immobilized at the tendon cell membrane.

Slit cleavage affects its distribution and stability

Next, we examined the distribution and stability of the Slit-myc tagged knocked-in proteins using anti-myc antibodies. Analysis of Slit-FL-myc embryos did not reveal specific labeling at the muscle attachment sites, nor did it show a signal in western blotting (Fig. 3A,F). This is consistent with Slit-FL-myc being cleaved,

and with degradation of the cleaved Slit-C-myc-tagged protein. Notably, staining was apparent in other tissues, e.g. along the heart cardioblasts, indicating that in these cells Slit-FL-myc is not rapidly degraded, or that it is produced at higher levels (supplementary material Fig. S2). Similarly, we did not detect myc labeling in embryos expressing knocked-in Slit-FL-CD8-myc (Fig. 3B), although it was clearly detected by western analysis (Fig. 3F). It was concluded that Slit-FL-CD8-myc is more stable than Slit-FL-myc; however, due to low expression levels by the tendon cells, it is not detected at these sites by fluorescent labeling.

The uncleavable version of Slit (Slit-UC-myc) was also undetectable at the tendon cell vicinity (Fig. 3C), and its overall levels were relatively low (Fig. 3F), suggesting that it diffuses and is rapidly degraded. Importantly, the uncleavable Slit that is membrane-bound (Slit-UC-CD8-myc) was clearly detected along the tendon cell membrane (Fig. 3D), in contrast to the cleavable membrane-bound Slit (Slit-CD8-myc, Fig. 3C), although their overall levels in the embryos are comparable (Fig. 3F). This confirms that membrane binding protects Slit from degradation. Because Slit-UC-CD8-myc rescued the *slit* mutant muscle phenotype (Fig. 2D), these results indicate that Slit accumulation at the tendon cell membrane is crucial for its function in proper guidance of LT and DA3 muscles. In addition, knock-in of the cleaved Slit-N-CD8-myc showed considerably higher myc staining along the tendon cell
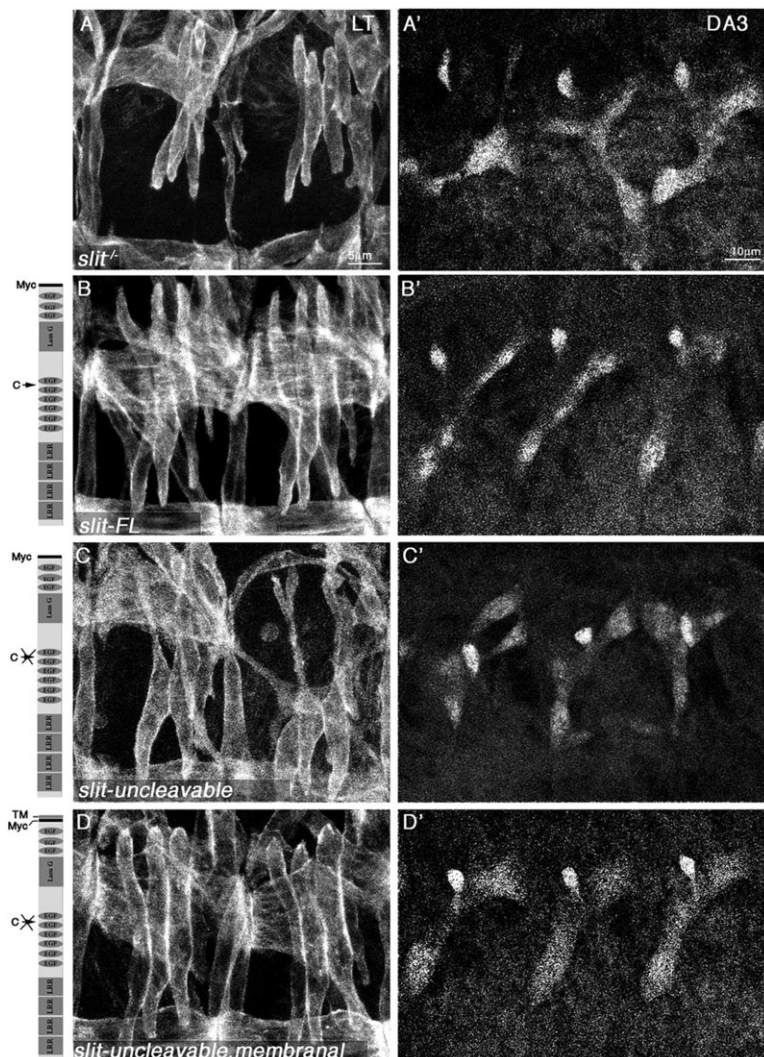

Fig. 2. Slit cleavage is essential for inducing the correct migration of LT and DA3 muscles. LT visualized with anti-tropomyosin (A,B,C,D) or DA3 muscles labeled with anti Collier (A′,B′,C′,D′) in *slit* mutant embryo (A,A′), *slit-FL* knocked into the *slit* locus (Slit-FL) (B,B′), *slit-uncleavable* knocked into the *slit* locus (Slit-UC) (C,C′) and *slit-uncleavable-membrane bound* knocked into the *slit* locus (Slit-UC membrane bound) (D,D′). All embryos are at stage 16. The corresponding schemes of Slit proteins are presented to the left of panels B,C,D. Scale bars: 5 µm in A-D; 10 µm in A′-D′.
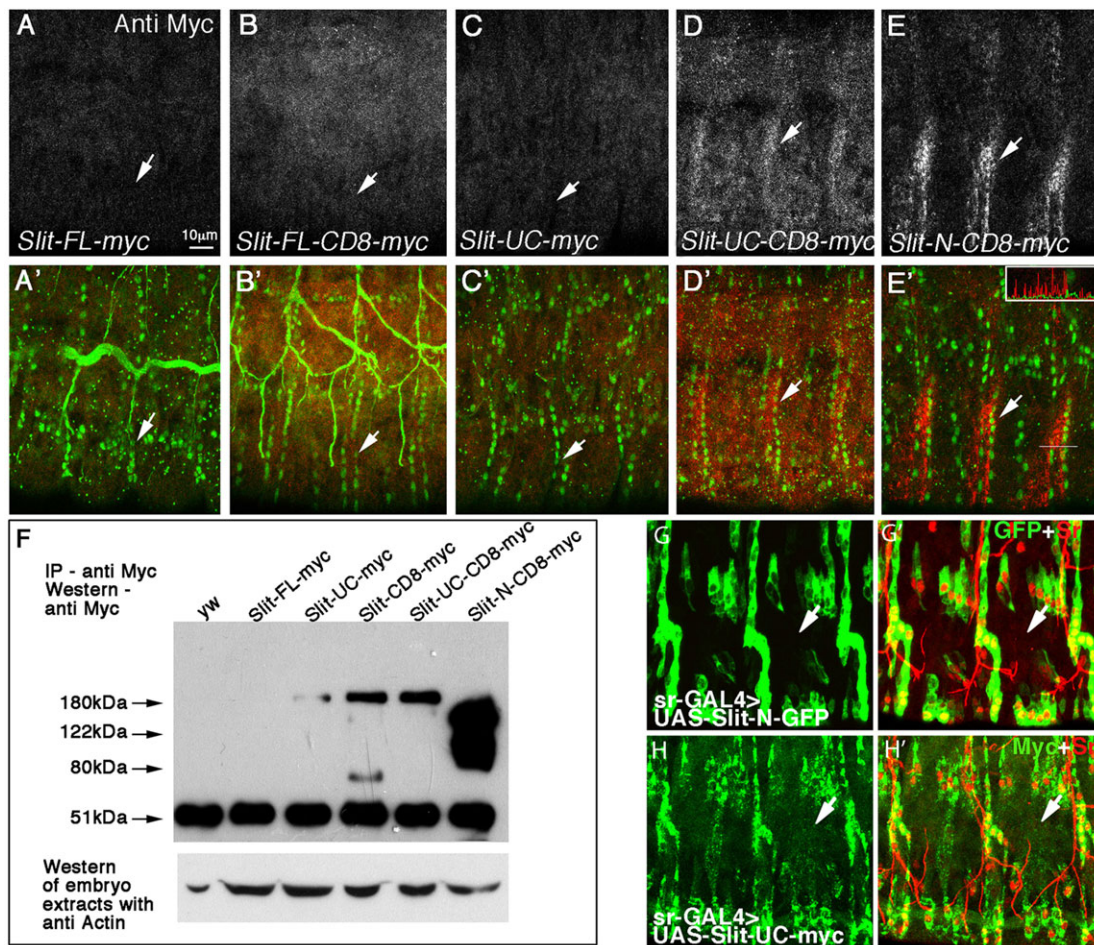
Fig. 3. Cleaved Slit-N is a highly stable non-diffusing protein. (A-E′) Staining with anti-myc antibody (red in A′,B′,C′,D′,E′ or white in A,B,C,D,E) of knocked-in slit-FL-myc (Slit-FL; A,A′), slit-FL-CD8-myc (B,B′), slit-uncleavable-myc (C,C′), slit-uncleavable-CD8 (D,D′) or slit-N′-CD8 (E,E′). Myc distribution, but not its levels, are presented. Tendon cells are marked with anti-Stripe (green, A′-E′). All embryos are at stage 16. White arrows indicate the segmental boundary tendon cells. The inset in E′ shows a line scan of Myc (red) and Stripe (green) profiles. (F) Immunoprecipitation of stage 16 embryo extract with anti-myc followed by western blotting with anti-myc. The ~52 kDa band represents the IgG heavy chain of the anti-myc antibody. Lower panel: western analysis of the embryo extracts taken for the myc IP, reacted with anti-actin. (G,G′) UAS-Slit-N-GFP driven by stripe-GAL4 and stained with anti-Stripe (red) and GFP (green). (H,H′) UAS-Slit-UC-myc driven by stripe-GAL4 and labeled with anti-Stripe (red) and myc (green). Arrows in G-H′ show regions devoid of tendon cells in which Slit-UC, but not Slit-N, is detected. Such dots are never observed with anti Myc staining of control embryo. Scale bar: 10 μm.

membrane (Fig. 3E), as well as more than 10-fold elevation in its protein levels relative to both Slit-FL-CD8 proteins (Fig. 3F). This result implies that Slit-N is significantly more stable than Slit-FL when both associate with the membrane. Interestingly, Slit-N-CD8-myc accumulated asymmetrically along the tendon cells (e.g. arrow in Fig. 3E′ and line scan in the inset). Such asymmetry may contribute to a differential effect of Slit on muscles reaching the tendon on both sides of the segmental border.

These experiments demonstrate that full-length Slit is an unstable protein; however, its cleaved N-terminal fragment is extremely stable. In addition, association with the membrane stabilizes both full-length and cleaved Slit.

To further analyze the distribution of the cleaved Slit-N polypeptide relative to uncleavable Slit, we overexpressed Slit-N-GFP or Slit-UC-myc in tendon cells (using the *sr-GAL4* driver) and compared their distributions. Whereas Slit-UC-myc diffused outside the tendon cell territory (Fig. 3H,H′), Slit-N-GFP remained associated with the tendon cell (Fig. 3G,G′), demonstrating that Slit-N, but not full-length Slit, associates with tendon cell surfaces. Taken together, these results demonstrate that, once produced by the tendon cell, Slit-N does not diffuse but

rather associates with the cell membrane, consistent with short-range Slit signaling by these cells.

Slit-N is a strong repellent signal

To address the outcome of accumulated active Slit-N on individual muscle migration, we followed the path of the LT muscles in embryos with knocked-in Slit-N-CD8 by live imaging. Interestingly, the mutant muscles lost the parallel dorsal-ventral orientation and elongated towards each other, producing unoriented aggregates (Fig. 4A-D; supplementary material Movie S5). Together with previous results, this behavior suggests that excessive repulsion by the segment borders from both sides pushes the muscles towards each other, implying that only low levels of repellent Slit signal allow the parallel dorsal-ventral extension of the LT muscles. Additional support for the repulsion activity of Slit-N was deduced from overexpression of Slit-N-GFP using two distinct drivers, *atonal-GAL4* and Hh-GAL4, in otherwise wild-type embryos. Muscles proximal to the cells expressing Slit-N-GFP avoided these cells, changing their orientation (Fig. 4, compare G,H with E,F and K,L with I,J). In the case of *atonal-GLA4*, 85% of the segments showed an aberrant pattern relative to 10% in control (*P*=0.00001).
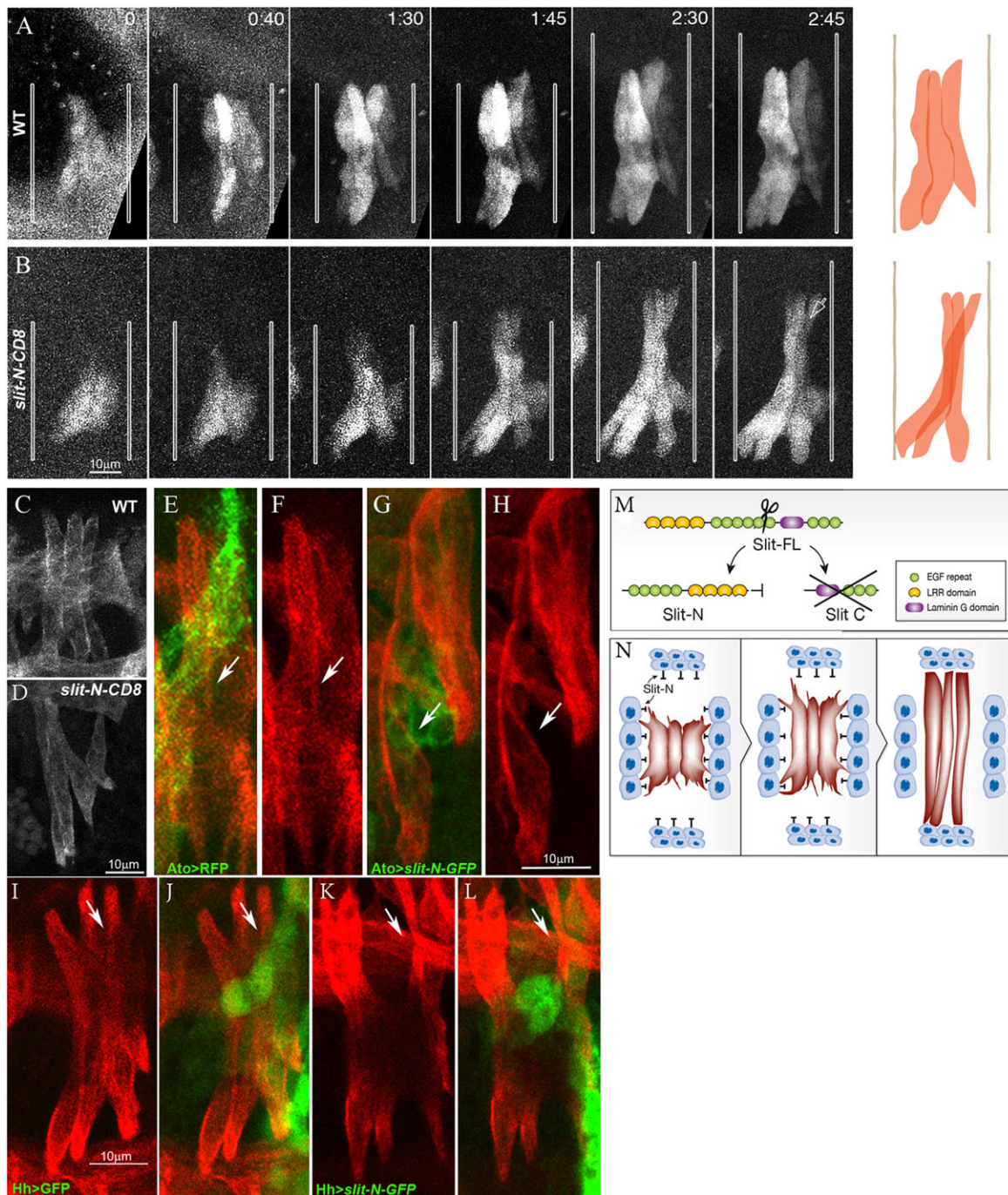
Fig. 4. Slit functions as a repellant for muscle elongation. (A,B) Live imaging of the LT muscles in wild type (A) or in embryos with knocked-in Slit-N-CD8 (B). (C,D) LT muscles in wild type (C) or in embryos expressing Slit-N-CD8 (D) after fixation. (E-H) Embryos overexpressing either UAS-RFP (green, E,F) or UAS-Slit-N-GFP (green, G,H) driven by *ato-GAL4* (arrows indicate the LT muscles). (I-L) Embryos overexpressing either UAS-GFP (green, J,L) or UAS-Slit-N-GFP (green, G,H) driven by *Hh-GAL4.* (M) Schematic representation of Slit cleavage. (N) A model describing how the repulsion by Slit-N produced by tendons orients muscle elongation. Scale bars: 10 µm.

To conclude, our findings show that the cleavage of Slit provides important regulation of its distribution, promoting its short-range signaling that is essential for exclusive repulsion of closely approaching muscles (see model in Fig. 4M,N). In contrast to a previous report, Slit appears to repel muscles, similar to its function in the nervous system. Whereas distinct muscles extend their leading edge in a muscle-specific inherited direction, Slit prevents mistaken routes and is essential for stopping muscles once they reach the target tendon site (Fig. 4N). Mechanistically, Slit cleavage transforms the protein into an active, stable polypeptide, which is tethered to the tendon cell, further protecting it from degradation and restricting its distribution. Whereas the nature of the protease that cleaves Slit has yet to be elucidated, the tendon-specific surface proteoglycans syndecan (Chanana et al., 2009; Coleman et al., 2010) and multiplexin (Harpaz et al., 2013; Meyer and Moussian, 2009; Momota et al., 2011, 2013), shown previously to bind Slit in the CNS or in the heart, respectively, might tether the cleaved Slit-N to the tendon cell membrane. This novel regulatory mechanism

controlling Slit distribution may also operate in other tissues, such as the heart and blood vessels, where Slit appears to be active between neighboring cells.

MATERIALS AND METHODS

Fly strains
Wild-type flies were *yw. mef2-GAL4, 69b-GAL4, sli²/CyO,Yfp, Yfp* strains were purchased from Bloomington Stock Center. Collier-GFP flies were a gift from Dr Alan Vincent (Centre de Biologie du Développement, UMR 5547 and IFR 109, CNRS and Université Paul Sabatier, France). Homozygous embryos were recognized by the lack of either CyO, YFP or CyO wg-lacZ. UAS-Slit-N-GFP and UAS-Slit-UC-Myc flies were a gift from Greg J. Bashaw (University of Pennsylvania, Philadelphia, USA). Ap-Me580-GFP flies were a gift from Mary Baylies (Memorial Sloan Kettering Cancer Center, New York, USA) (Folker et al., 2012, 2014). Slit knock-in lines included: Slit full-length, Slit-FL/CyO wg-lacZ; Slit-uncleavable, Slit-UC/CyO wg-lacZ; Slit-membrane bound Slit, CD8/CyO wg-lacZ; Slit-membrane bound uncleavable, Slit-UC-CD8/CyO wg-lacZ; and Slit-N terminal fragment, Slit-N/CyO wg-lacZ.

Antibodies
Mouse anti-Collier (1:200) (Dubois et al., 2007) was a gift from Dr Alan Vincent (Centre de Biologie du Développement, Toulouse, France). Other antibodies included rat anti-tropomyosin (1:400, Abcam), chicken anti-β-galactosidase (1:400, Abcam), chicken anti-GFP (Aves Labs), guinea pig anti-Stripe (1:400) (our lab), chicken anti-HA (1:400), mouse anti-HA (Covance MMs-101p, 1:400), mouse anti-myc and mouse anti-Slit (1:30, Hybridoma Bank). Secondary fluorescent antibodies were purchased from Jackson Laboratories.

Immunostaining
Staged embryos were collected and fixed as previously described (Ashburner et al., 2005). Embryos were visualized with a Zeiss LSM710 confocal system, and images were processed using Adobe Photoshop.

Live imaging
Staged embryos were dechorionated, selected using a fluorescent stereoscope, arranged, covered with Halocarbon oil 700 (H8898, Sigma-Aldrich, USA) and visualized with a Zeiss LSM710 confocal system. The time series were transformed into a film using ImageJ software.

Western blot and immunoprecipitation
Staged embryos were collected and protein extract was produced in RIPA buffer. The soluble extract was separated on a 7% denaturing gel, blotted onto nitrocellulose and reacted with mouse anti-Slit (1:1000, Hybridoma Bank) and HRP-conjugated anti-mouse. The signal was visualized using Thermo Scientific Supersignal. For immunoprecipitation, embryo protein extracts containing equivalent amounts of protein were reacted with beads conjugated with anti-myc antibodies, washed and then boiled in sample buffer.

Statistical analysis
Segments were scored separately and the fraction of mutant segments for each genetic background was calculated. The significance of the effect was calculated using the following test:

$$z = \frac{\hat{\pi}_1 - \hat{\pi}_2}{\sigma_{\hat{\pi}_1 - \hat{\pi}_2}},$$

where $\sigma_{\hat{\pi}_1 - \hat{\pi}_2} = \sqrt{\pi(1-\pi)\left(\frac{1}{n_1} + \frac{1}{n_2}\right)}.$

Author contributions
E.O. and T.V. developed the concepts, E.O. performed the experiments and data analysis, T.V. prepared the manuscript, M.B., B.D. and F.S. provided the Slit knock-in flies.

Supplementary material
Supplementary material available online at
http://dev.biologists.org/lookup/suppl/doi:10.1242/dev.119131/-/DC1

References
Ashburner, M., Golic, K. G. and Hawley, R. S. (2005). *Drosophila: A Laboratory Handbook*, 2nd edn. Cold Spring Harbor, NY: Cold Spring Harbor Laboratory Press.

Bökel, C. and Brown, N. H. (2002). Integrins in development: moving on, responding to, and sticking to the extracellular matrix. *Dev. Cell* **3**, 311-321.

Brose, K., Bland, K. S., Wang, K. H., Arnott, D., Henzel, W., Goodman, C. S., Tessier-Lavigne, M. and Kidd, T. (1999). Slit proteins bind Robo receptors and have an evolutionarily conserved role in repulsive axon guidance. *Cell* **96**, 795-806.

Chanana, B., Steigemann, P., Jackle, H. and Vorbruggen, G. (2009). Reception of Slit requires only the chondroitin-sulphate-modified extracellular domain of Syndecan at the target cell surface. *Proc. Natl. Acad. Sci. USA* **106**, 11984-11988.

Coleman, H. A., Labrador, J.-P., Chance, R. K. and Bashaw, G. J. (2010). The Adam family metalloprotease Kuzbanian regulates the cleavage of the roundabout receptor to control axon repulsion at the midline. *Development* **137**, 2417-2426.

Dubois, L., Enriquez, J., Daburon, V., Crozet, F., Lebreton, G., Crozatier, M. and Vincent, A. (2007). Collier transcription in a single Drosophila muscle lineage: the combinatorial control of muscle identity. *Development* **134**, 4347-4355.

Folker, E. S., Schulman, V. K. and Baylies, M. K. (2012). Muscle length and myonuclear position are independently regulated by distinct Dynein pathways. *Development* **139**, 3827-3837.

Folker, E. S., Schulman, V. K. and Baylies, M. K. (2014). Translocating myonuclei have distinct leading and lagging edges that require kinesin and dynein. *Development* **141**, 355-366.

Harpaz, N., Ordan, E., Ocorr, K., Bodmer, R. and Volk, T. (2013). Multiplexin promotes heart but not aorta morphogenesis by polarized enhancement of slit/robo activity at the heart lumen. *PLoS Genet.* **9**, e1003597.

Kidd, T., Bland, K. S. and Goodman, C. S. (1999). Slit is the midline repellent for the robo receptor in Drosophila. *Cell* **96**, 785-794.

Kramer, S. G., Kidd, T., Simpson, J. H. and Goodman, C. S. (2001). Switching repulsion to attraction: changing responses to slit during transition in mesoderm migration. *Science* **292**, 737-740.

Meyer, F. and Moussian, B. (2009). Drosophila multiplexin (Dmp) modulates motor axon pathfinding accuracy. *Dev. Growth Differ.* **51**, 483-498.

Momota, R., Naito, I., Ninomiya, Y. and Ohtsuka, A. (2011). Drosophila type XV/XVIII collagen, Mp, is involved in Wingless distribution. *Matrix Biol.* **30**, 258-266.

Momota, R., Narasaki, M., Komiyama, T., Naito, I., Ninomiya, Y. and Ohtsuka, A. (2013). Drosophila type XV/XVIII collagen mutants manifest integrin mediated mitochondrial dysfunction, which is improved by cyclosporin A and losartan. *Int. J. Biochem. Cell Biol.* **45**, 1003-1011.

Nguyen Ba-Charvet, K. T., Brose, K., Ma, L., Wang, K. H., Marillat, V., Sotelo, C., Tessier-Lavigne, M. and Chedotal, A. (2001). Diversity and specificity of actions of Slit2 proteolytic fragments in axon guidance. *J. Neurosci.* **21**, 4281-4289.

Rothberg, J. M. and Artavanis-Tsakonas, S. (1992). Modularity of the slit protein: characterization of a conserved carboxy-terminal sequence in secreted proteins and a motif implicated in extracellular protein interactions. *J. Mol. Biol.* **227**, 367-370.

Rothberg, J. M., Hartley, D. A., Walther, Z. and Artavanis-Tsakonas, S. (1988). slit: an EGF-homologous locus of D. melanogaster involved in the development of the embryonic central nervous system. *Cell* **55**, 1047-1059.

Rothberg, J. M., Jacobs, J. R., Goodman, C. S. and Artavanis-Tsakonas, S. (1990). slit: an extracellular protein necessary for development of midline glia and commissural axon pathways contains both EGF and LRR domains. *Genes Dev.* **4**, 2169-2187.

Schejter, E. D. and Baylies, M. K. (2010). Born to run: creating the muscle fiber. *Curr. Opin. Cell Biol.* **22**, 566-574.

Schnorrer, F. and Dickson, B. J. (2004). Muscle building: mechanisms of myotube guidance and attachment site selection. *Dev. Cell* **7**, 9-20.

Schweitzer, R., Zelzer, E. and Volk, T. (2010). Connecting muscles to tendons: tendons and musculoskeletal development in flies and vertebrates. *Development* **137**, 2807-2817.

Wang, K. H., Brose, K., Arnott, D., Kidd, T., Goodman, C. S., Henzel, W. and Tessier-Lavigne, M. (1999). Biochemical purification of a mammalian slit protein as a positive regulator of sensory axon elongation and branching. *Cell* **96**, 771-784.

Wayburn, B. and Volk, T. (2009). LRT, a tendon-specific leucine-rich repeat protein, promotes muscle-tendon targeting through its interaction with Robo. *Development* **136**, 3607-3615.
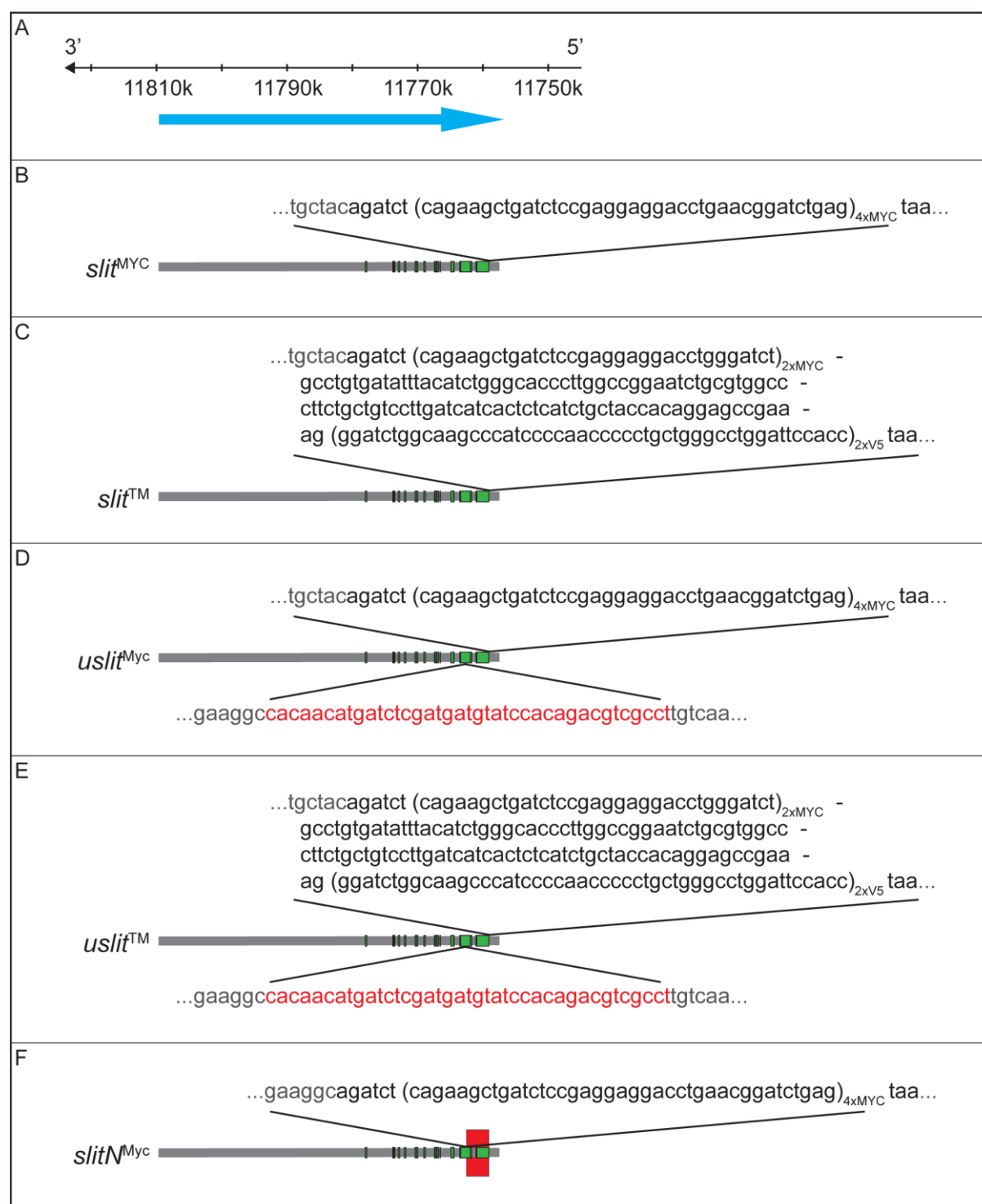
DEVELOPMENT

Supplemental Figures

Figure S1: The production of Slit knocked-in constructs (related to Figure 2)

Five new *slit* alleles were generated using the "hands in" homologous recombination technique. Shown is the annotated position (in bp) of the endogenous *slit* locus; blue arrow indicates the *slit* reading frame (A). *slit*^MYC (B), *slit*^TM (C), *uslit*^MYC (D), *uslit*^TM (E) and

slitN^{MYC} (F) loci are depicted as grey lines or grey-labeled sequence blow-ups; coding exons are marked with green bars. Black-labeled sequences indicate in-frame fusions with a MYC tag tetramer (B,D,F) or a 2xMYC-cd8TM-2xV5 membrane anchor (C,E), respectively. The red-labeled (D,E) or red-boxed sequences (F) indicate deleted endogenous *slit* sequence sections.
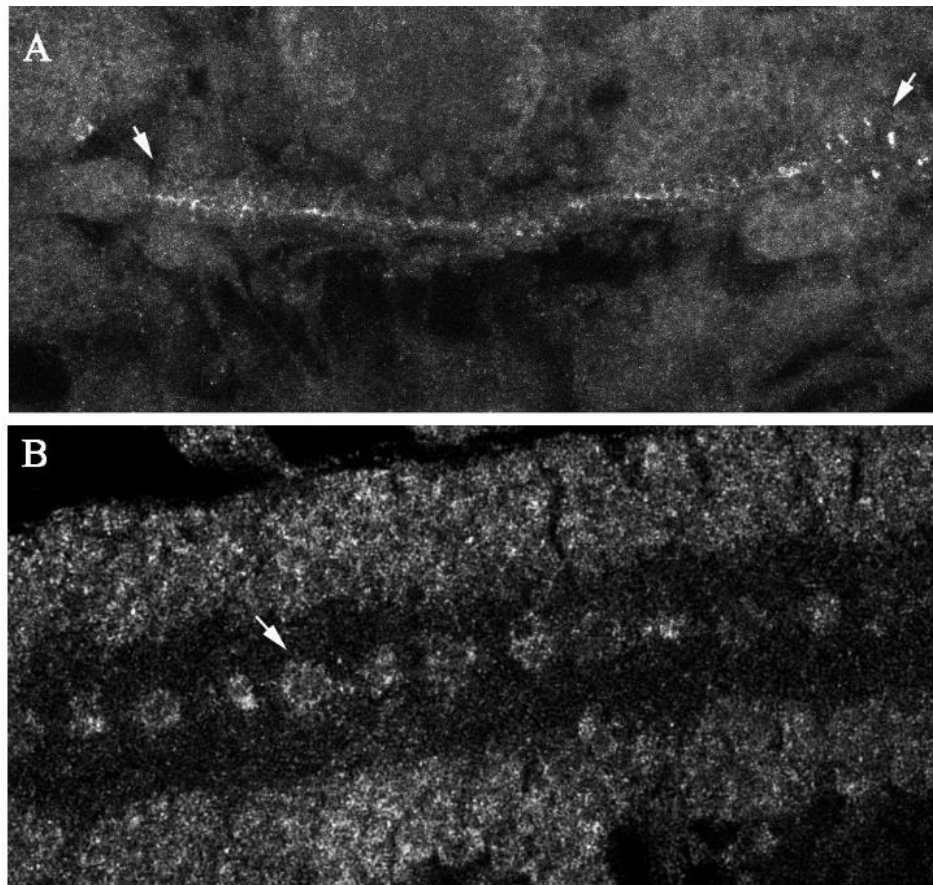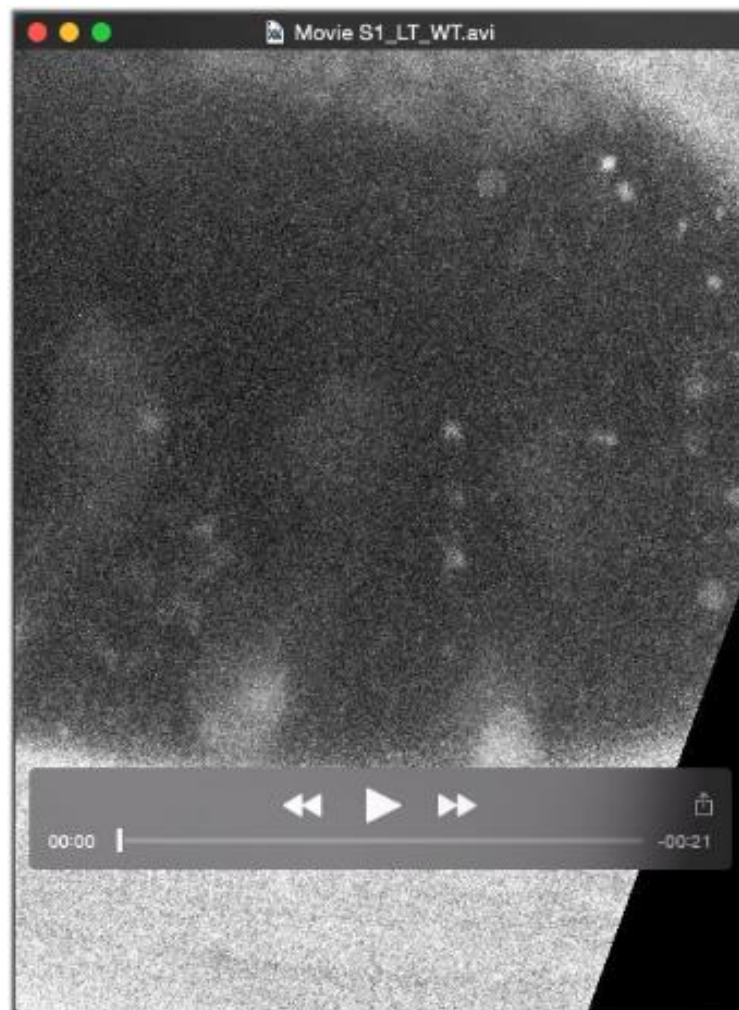
Figure S2: Staining of Slit-FL-myc (related to Figure 3)

(A) Dorsal view of an embryo carrying Slit-FL-myc and labeled with anti-myc antibody. The entire dorsal vessel is clearly labeled (arrows mark its beginning and end). (B) Ventral view of a similar embryo showing labeling of the midline glia (arrow marks a single midline glia cell).
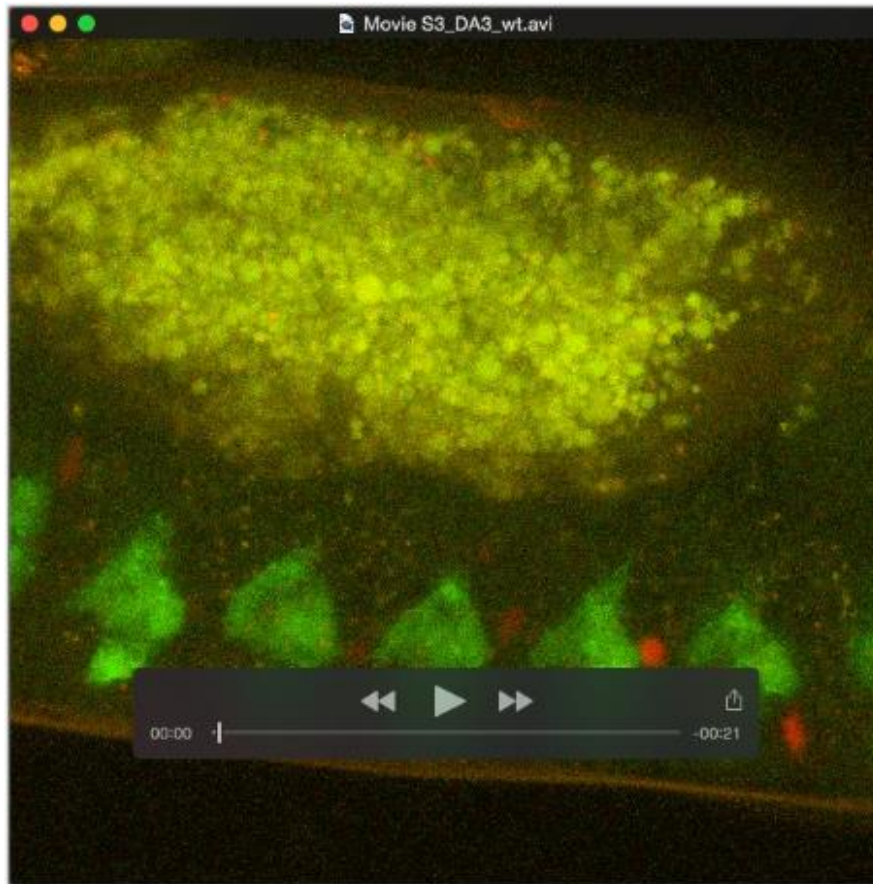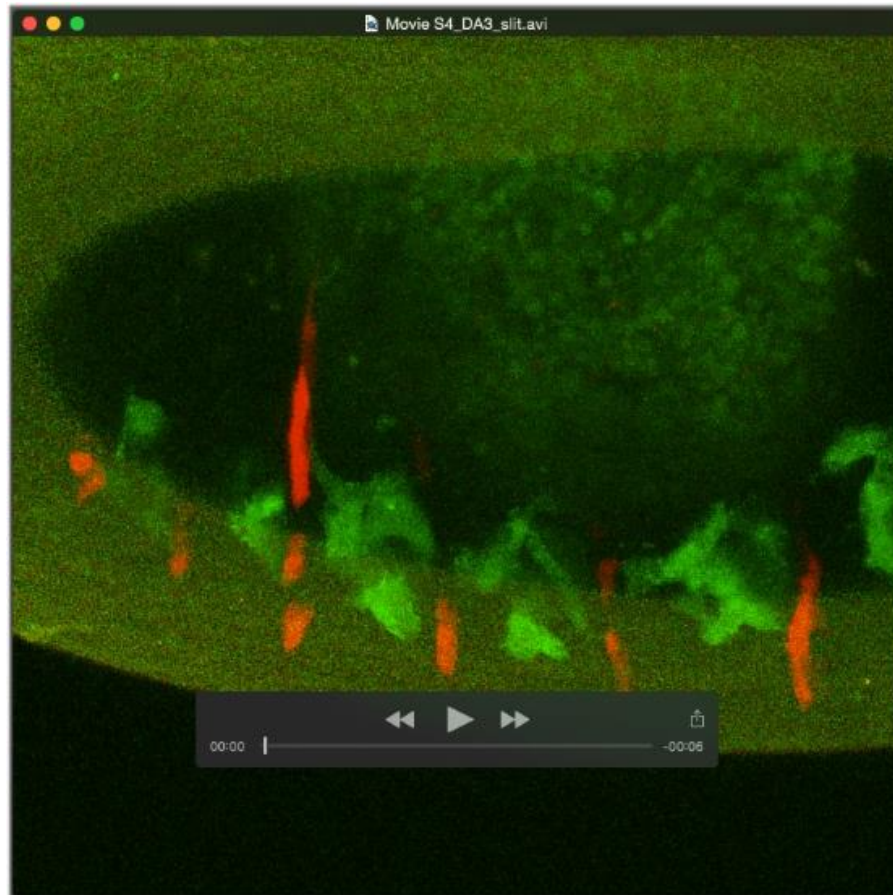
Supplemental Movies

Movie S1: Migration of fluorescently-labeled LT muscles in WT embryo. Related to Figure 1.
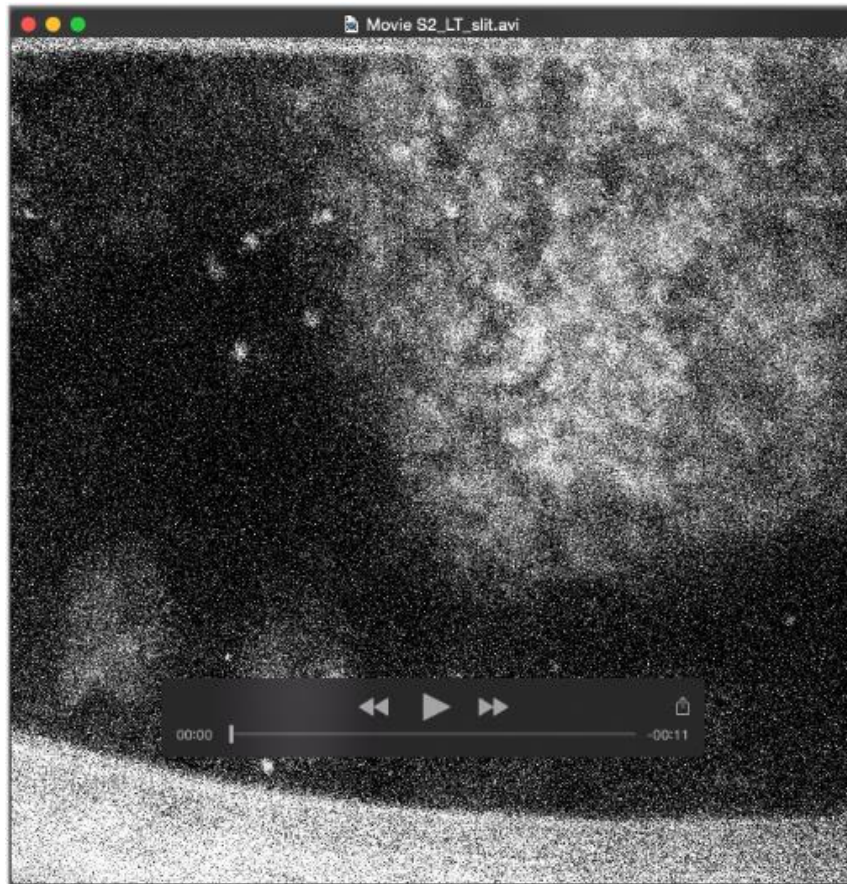
Movie S2: Migration of fluorescently-labeled LT muscles in *slit* mutant embryo. Related to Figure 1.

Movie S3: Migration of the DA3 muscle (labeled with GFP) relative to the tendon cells (labeled with RFP) in WT embryos. Related to Figure 1.

Movie S4: Migration of the DA3 muscle (labeled with GFP) relative to the tendon cells (labeled with RFP) in *slit* mutant embryos. Related to Figure 1.

Movie S5: Migration of fluorescently-labeled LT muscles in Slit-N-CD8 knock-in embryo. Related to Figure 4.